GVE-Based Dynamics and Control for Formation Flying Spacecraft

Louis Breger* and Jonathan P. How†

MIT Department of Aeronautics and Astronautics

Formation flying is an enabling technology for many future space missions. This paper presents extensions to the equations of relative motion expressed in Keplerian orbital elements, including new initialization techniques for general formation configurations. A new linear time-varying form of the equations of relative motion is developed from Gauss' Variational Equations and used in a model predictive controller. The linearizing assumptions for these equations are shown to be consistent with typical formation flying scenarios. Several linear, convex initialization techniques are presented, as well as a general, decentralized method for coordinating a tetrahedral formation using differential orbital elements. Control methods are validated using a commercial numerical propagator.

I. Introduction

In spacecraft formation flying mission design, it is generally true that the control of relative spacecraft states is more important than the control of absolute states. In addition, knowledge of the relative states of spacecraft in a formation is often far more accurate than knowledge of the formation's absolute state. For these reasons, formation control objectives are typically focused on controlling the relative states of the spacecraft. Variants of Hill's and Lawden's equations of relative motion have been used for online planning and control.[24] Both of these approaches linearize the nonlinear dynamics of orbital motion about a reference orbit. However, the linearization approach taken in those cases restricts the separation distances of the satellites in the formation. For larger separation distances, the equations of motion can no longer be used to cancel relative drift rates (initialization) or to accurately predict the effect of inputs (control).[12] In the case of the MMS mission, four spacecraft will be placed in a tetrahedron-shaped relative configuration that will have sides ranging between 10–1000 km. These separations far exceed the distances for which Hill's and Lawden's models are valid, even with the correction terms introduced in Ref. 24.

Another approach that often appears in the literature is formation control using Gauss' Variational Equations (GVEs).[6,7,8,14] GVEs have been used for many years to account for perturbations in orbits arising from drag and Earth oblateness effects, as well as to design Lyapunov and fixed impulse control systems.[16] GVEs are convenient for specifying and controlling widely separated formations because they are linearized about orbital elements, which are expressed in a curvilinear frame in which large rectilinear distances can be captured by small element perturbations. In addition, the GVEs provide a computationally simple way (no frame rotations are required) to obtain linearized dynamics about the orbits of each spacecraft in the formation. This bypasses the linearization error created by representing the entire formation in a single rectilinear frame, which was the approach used in Ref. 5. The use of GVE dynamics as opposed to Hill's dynamics incurs the cost of computation associated with the use of multiple sets of time-varying equations of motion. Specifying a formation's relative geometry in terms of differential orbital elements is an exact approach that does not degrade for large spacecraft separations. However, the advantage of using GVEs for control could be reproduced by using a separate Lawden's frame for each spacecraft in the formation while still using orbital element differences to represent the formation relative geometry. Given that a nonlinear transformation and rotation is required to switch between a Lawden's frame and orbital element differences, and that GVEs are already linearized in an orbital element frame, it is both simpler and computationally more efficient to use orbital element differences to specify the formation configuration and GVEs for control.

*Research Assistant, MIT Department of Aeronautics and Astronautics, lbreger@mit.edu

†Associate Professor, MIT Department of Aeronautics and Astronautics, jhow@mit.edu

Several research groups have proposed control laws for formation-flying spacecraft that use GVEs to design impulsive thrusting maneuvers for orbit correction. For example, Ref. 14 proposes an general orbit correction scheme that uses GVEs to develop four impulsive thrusts that are applied at fixed points in an orbit. This four-impulse method is not guaranteed to be fuel-optimal and the approach presented in this paper consistently produces trajectories that require less fuel to accomplish identical goals. A method of producing optimized four-impulse plans for very-low eccentricity orbits is presented in Ref. 10, but this approach does not extend to the higher eccentricities required for MMS missions. Another method based on GVEs[8] allows optimized planning for low Earth orbits, but only permits optimization over a single impulsive thrust, guaranteeing that the solution will be sub-optimal in many cases. In addition, this approach is only derived for correcting errors in semimajor axis, eccentricity, and inclination. Another approach to using GVEs for formation control is to derive a continuous proportional-derivative controller satisfying a Lyapunov equation.[6,7,9,13]

This paper presents a formation flying spacecraft control approach using GVEs as the dynamics in a model predictive control system. A novel aspect of this approach is the use of the GVEs to optimize the control inputs, or equivalently the spacecraft trajectory, over a set time-horizon. Plans are regularly re-optimized, forming a closed-loop system. By extending previous planning approaches to use GVEs, we can optimize the plans for spacecraft in widely-separated, highly elliptic orbits. Results are presented to show that the GVE-based planning system is more fuel-efficient than both the four-impulse method in Ref. 14 and the single-impulse optimized method in Ref. 8. In addition control optimized online has the advantage of being capable of handling many types of constraints, such as limited thrust capability, sensor noise robustness, and error box maintenance.[5] This paper also presents a method for optimizing the initialization of the tetrahedron formation using relative orbital elements, which allows for rotation and translation of the formation. We also extend the virtual center approach to formation flying in Ref. 11 to GVEs and present a decentralized implementation.

Gauss' Variational Equations (GVEs) are derived in Ref. 16 and are reproduced here for reference

$$\frac{d}{dt}\begin{pmatrix} a \\ e \\ i \\ \Omega \\ \omega \\ M_0 \end{pmatrix} = \begin{pmatrix} 0 \\ 0 \\ 0 \\ 0 \\ 0 \\ n \end{pmatrix} + \begin{pmatrix} \frac{2a^2 e \sin f}{h} & \frac{2a^2 e \sin f}{h} & 0 \\ \frac{p \sin f}{h} & \frac{(p+r)\cos f + re}{h} & 0 \\ 0 & 0 & \frac{r\cos\theta}{h} \\ 0 & 0 & \frac{r \sin\theta}{h \sin i} \\ -\frac{p\cos f}{he} & \frac{(p+r)\sin f}{he} & -\frac{r\sin\theta\cos i}{h\sin i} \\ \frac{b(p\cos f - 2re)}{ahe} & -\frac{b(p+r)\sin f}{ahe} & 0 \end{pmatrix} \begin{pmatrix} \mathbf{u_r} \\ \mathbf{u}_\theta \\ \mathbf{u_h} \end{pmatrix} \tag{1}$$

where the state vector elements are a (semimajor axis), e (eccentricity), i (inclination), Ω (right ascension of the ascending node), ω (argument of periapse), and M_0 (mean motion). The other terms in the variational expression are p (semi-latus rectum), b (semiminor axis), h (angular momentum), θ (argument of latitude), r (magnitude of radius vector), and n (mean motion). All units are in radians, except for semimajor axis and radius (meters), angular momentum (kilogram $\cdot$ meters^2 per second), mean motion (1/seconds), and eccentricity (dimensionless). The input acceleration components $\mathbf{u_r}$, $\mathbf{u}_\theta$, and $\mathbf{u_h}$ are in the radial, in-track, and cross-track directions, respectively, of an LVLH frame centered on the satellite and have units of meters per second^2. The form of the GVEs can be more compactly expressed as

$$\dot{\mathbf{e}} = A(\mathbf{e}) + B(\mathbf{e})\mathbf{u} \tag{2}$$

where $\mathbf{e}$ is the state vector in Eq. 1, $B(\mathbf{e})$ is the input effect matrix, $\mathbf{u}$ is the vector of thrust inputs in the radial, in-track, and cross-track directions, and $A(\mathbf{e}) = (\ 0 \quad 0 \quad 0 \quad 0 \quad 0 \quad \sqrt{\mu/a^3}\ )^T$, where μ is the gravitational parameter.

II. Previous Approaches to Control Using GVEs

A common approach when basing control on GVE dynamics is to use a nonlinear PD-based Lyapunov regulator of the form

$$\mathbf{u} = -KB(\mathbf{e})^T\zeta \tag{3}$$

where ζ is the current orbital element offset from the reference orbit $\mathbf{e}$ and K is a constant positive definite matrix.[6,7,9,13] Control algorithms of this type have been shown to be asymptotically stable in most cases,[9] but belong to a class of control systems that fire continuously. Continuous firing is generally not desirable

for space missions because it is often disruptive to the science mission, it typically must be coupled with attitude maneuvers, and it expends fuel (nonreplenishable aboard a spacecraft) continuously.

Another approach to differential element control is presented in Ref. 14. In that approach, it is observed that the GVEs decouple at several points during an orbit. By exploiting the decoupling points, an algorithm requiring a maximum of four impulsive thrusts is proposed. This approach is simple in an algorithmic sense, but requires a fixed time period (*i.e.,* one orbit) to correct state errors and is not guaranteed to be fuel-optimal (or even near-fuel-optimal). Ref. 8 presents another method of formation control based on GVEs that uses a single corrective thrust that is optimized nonlinearly. Although this method is guaranteed to find the optimal single-thrust correction for an arbitrary time period, it is not guaranteed (or likely) to find the optimal multiple-thrust correction. In addition, this approach is restricted to use in low Earth orbits and is only designed to correct errors in semimajor axis, eccentricity, and inclination. An approach presented in Ref. 15 uses a pseudo-inverse to the GVE control effect matrix to calculate a single corrective impulse. This approach is not guaranteed to be fuel-optimal for any cases and is not accurate for correcting position errors.

In contrast, this section describes a control law that generally does not fire continuously and makes explicit its objective to minimize fuel use. The control approach utilizes the linearized relative dynamics of Gauss' Variation Equations to optimize the effects of arbitrarily many inputs over a chosen planning horizon. The next section examines the validity of using a linearized relative form of the equations of satellite motion based on GVEs.

III. Relative Orbital Elements and Linearization Validity

In a formation, the orbital element state of the ith satellite is denoted $\mathbf{e}_i$. The states of the vehicles in the formation can be specified by relative orbital elements by subtracting the state of an arbitrarily chosen spacecraft in the formation ($\mathbf{e}_1$)

$$\delta\mathbf{e}_i = \mathbf{e}_i - \mathbf{e}_1 \tag{4}$$

For a desired orbit geometry, a set of desired relative elements, $\delta\mathbf{e}_{di}$ will specify the desired state $\mathbf{e}_{di}$ of each spacecraft in the formation

$$\mathbf{e}_{di} = \mathbf{e}_1 + \delta\mathbf{e}_{di} \tag{5}$$

The state error for the ith spacecraft in the formation, ζ_i, is then defined as

$$\zeta_i = \mathbf{e}_i - \mathbf{e}_{di} = \delta\mathbf{e}_i - \delta\mathbf{e}_{di} \tag{6}$$

The form of Gauss' Variational Equations in Eq. 1 is for perturbations of orbital elements. To reformulate these equations for perturbations of relative orbital elements,[13] the GVEs for $\mathbf{e}_i$ and $\mathbf{e}_{di}$ are placed together

$$\dot{\zeta}_i = \dot{\mathbf{e}}_i - \dot{\mathbf{e}}_{di} = A(\mathbf{e}_i) - A(\mathbf{e}_{di}) + B(\mathbf{e}_i)\mathbf{u}_i \tag{7}$$

where the term $B(\mathbf{e}_{di})\mathbf{u}_{di}$ has been excluded because thrusting only occurs at the point of the spacecraft, not at its desired state, which is assumed to be a constant Keplerian orbit. The unforced dynamics can be linearized by introducing the first order approximation

$$A(\mathbf{e}_i) - A(\mathbf{e}_{di}) \simeq \left.\frac{\partial A}{\partial \mathbf{e}}\right|_{\mathbf{e}_{di}} (\mathbf{e}_i - \mathbf{e}_{di}) = \left.\frac{\partial A}{\partial \mathbf{e}}\right|_{\mathbf{e}_{di}} \zeta_i \equiv A^*(\mathbf{e}_{di})\zeta_i \tag{8}$$

where the matrix $A^*(\mathbf{e}_{di})$ is all zeros except for the lower-leftmost element, which is $-3n/2a$. With this approximation, the differential GVE expression can be rewritten as

$$\dot{\zeta}_i = A^*(\mathbf{e}_{di})\zeta_i + B(\mathbf{e}_i)\mathbf{u}_i = A^*(\mathbf{e}_{di})\zeta_i + B(\mathbf{e}_{di} + \zeta_i)\mathbf{u}_i \tag{9}$$

In this case the control of the relative error state, ζ_i, is nonlinear, because the control effect matrix B is a function of the state. Ref. 13 accounts for this nonlinearity in a continuous nonlinear control law that was proven to be asymptotically stable. The control approach developed in this section uses linearized dynamics to predict the effect of future control inputs. Linearizing the matrix B in Eq. 9 yields

$$\dot{\zeta}_i \simeq A^*(\mathbf{e}_{di})\zeta_i + \left(B(\mathbf{e}_{di}) + \left.\frac{\partial B}{\partial \mathbf{e}}\right|_{\mathbf{e}_{di}} \zeta_i\right)\mathbf{u}_i = A^*(\mathbf{e}_{di})\zeta_i + B(\mathbf{e}_{di})\mathbf{u}_i + [B^*(\mathbf{e}_{di})]\zeta_i\mathbf{u}_i \tag{10}$$

where the term $B^*(\mathbf{e}_{di})$ is a third rank tensor and the quantity $B^*(\mathbf{e}_{di})\zeta_i$ is a matrix with the same dimensions as $B(\mathbf{e}_{di})$. For convenience, define

$$\Delta B \equiv B^*(\mathbf{e}_{di})\zeta_i \tag{11}$$

resulting in the new state equation

$$\dot{\zeta}_i = A^*(\mathbf{e}_{di})\zeta_i + (B(\mathbf{e}_{di}) + \Delta B)\,\mathbf{u}_i \tag{12}$$

Note that if ΔB is much smaller than $B(\mathbf{e}_{di})$, then the first order term can safely be ignored, yielding the linearized system

$$\dot{\zeta}_i = A^*(\mathbf{e}_{di})\zeta_i + B(\mathbf{e}_{di})\mathbf{u}_i \tag{13}$$

which can be controlled using any one of a variety of linear control techniques, including the model predictive controller discussed in Section IV.

The critical requirement for linear control and planning is that the term ΔB holds much less influence on the state than the term $B(\mathbf{e}_{di})$. However, ΔB is a linear function of the state error ζ_i, which can be arbitrarily large. The amount of acceptable error due to linearization will be a function of the mission scenario, but the linearization assumption will typically only be valid for small values of the state error. A bound on the magnitude of this error can be developed by comparing the induced norm of the difference between the control influence matrix at its desired state, $B(\mathbf{e}_{di})$ and at the actual position of the spacecraft, $B(\mathbf{e}_i)$. In Eq. 11, the first order approximation of this term was defined as ΔB. In the following examples, ΔB_{true}, which is defined as

$$\Delta B_{\text{true}} = B(\mathbf{e}_i) - B(\mathbf{e}_{di}) \tag{14}$$

and will be calculated numerically. The cutoff point of acceptable linearization error is when the norm of ΔB exceeds some (mission dependent) fraction of the norm of $B(\mathbf{e}_{di})$.

To investigate this cutoff point, the following examples consider many random values of ζ_i in the set $\|\zeta_i\|_2 = r$ and calculate ΔB_{true}. The ΔB_{true} with the largest 2-norm will be used to test the validity of the linearization for a given r. This procedure is repeated for multiple r to find the largest $\|\zeta\|_2$ for which the linearization is considered valid.

Example: Low Earth Orbit – An example low Earth orbit is

$$\mathbf{e}_{di} = \begin{pmatrix} 1.08182072 & 0.005000000 & 0.610865238 & 2\pi & \pi & 3.82376588 \end{pmatrix}^T \tag{15}$$

where the first element, semimajor axis, is normalized by the Earth's radius, making the orbital element vector dimensionless. The matrix corresponding $B(\mathbf{e}_{di})$ is

$$B(\mathbf{e}_{di}) = \begin{pmatrix} -5.6794478 & 1808.6011 & 0 \\ -0.000082308780 & -0.00020502572 & 0 \\ 0 & 0 & 0.00010304404 \\ 0 & 0 & 0.00014406293 \\ 0.020528419 & -0.032987976 & -0.00011800944 \\ -0.020792326 & 0.032987564 & 0 \end{pmatrix} \tag{16}$$

where $\|B(\mathbf{e}_{di})\|_2 = 1808.61$. The effect of perturbing $\mathbf{e}_{di}$ for a given norm bound on ζ_i is shown in Figure 1. The figure shows that for a linearization validity cutoff of 0.1, where $\|\Delta B(\mathbf{e}_{di}, \zeta)_{\text{true}}\|_2 \leq 0.1\|B(\mathbf{e}_{di})_{\text{true}}\|_2$, can be achieved by observing the bound $\|\zeta\|_2 \leq 0.08$. This choice of bound allows for orbital element perturbations that equate to rectilinear distances on the order of 275 kilometers and velocities on the order of 416 meters per second. Since typical error box sizes for LEO formation flying missions are between 10–1000 meters in size, the linearization should be a valid approximation for most missions of interest.

Example: Highly Elliptical Earth Orbit – One motivation for using GVEs as the linearized dynamics in a planner is recent interest in widely spaced, highly elliptical orbits.[20] An orbit of this type is

$$\mathbf{e}_{di} = \begin{pmatrix} 6.59989032 & 0.818181000 & 0.174532925 & 2\pi & 0 & \pi \end{pmatrix}^T \tag{17}$$

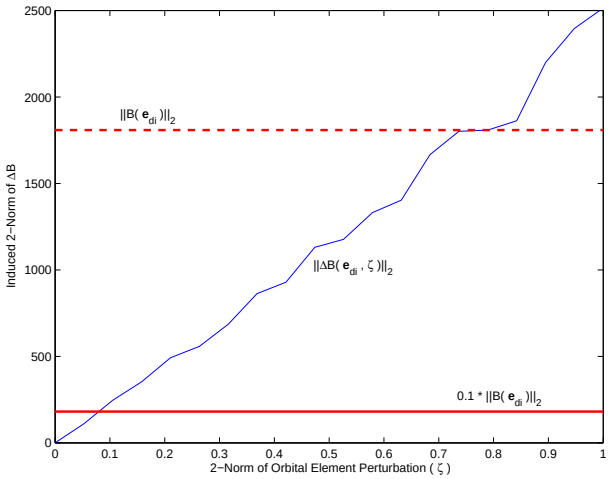

Fig. 1: Effect of Orbital Element Perturbations on the ΔB_{true} Matrix for a LEO Orbit

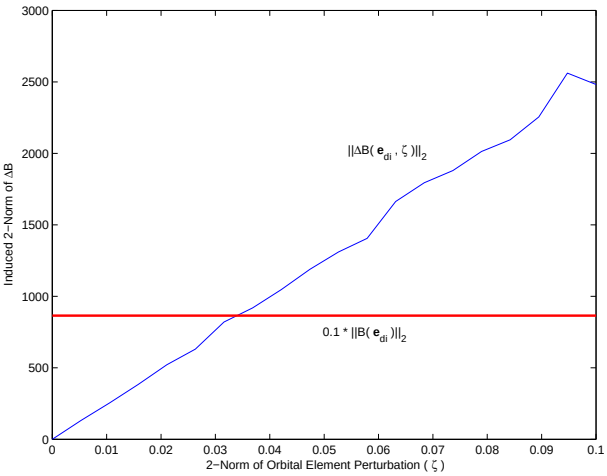

Fig. 2: Effect of Orbital Element Perturbations on the ΔB_{true} Matrix for a HEO Orbit

with

$$B(\mathbf{e}_{di}) = \begin{pmatrix} 4.767920 \times 10^{-12} & 8651.830 & 0 \\ 2.288208 \times 10^{-20} & -0.0003736926 & 0 \\ 0 & 0 & -0.001027650 \\ 0 & 0 & 7.247461 \times 10^{-19} \\ 0.0002283680 & 1.817849 \times 10^{-19} & -7.137356 \times 10^{-19} \\ -0.001313020 & -1.45192 \times 10^{-19} & 0 \end{pmatrix} \tag{18}$$

Repeating the same procedure used for the LEO case, it is determined from Figure 2 that for a 10% linearization validity cutoff, the bound which must be observed is $\|\zeta\|_2 \leq 0.034$. In this case, the bound on $\|\zeta\|_2$ corresponds to rectilinear distances of approximately 460 kilometers and velocities of 18.5 meters per second. As in the LEO case, these distances are far larger than expected error box sizes (*i.e.,* expected distances over which control would be planned). Unlike the LEO case, error boxes for widely-separated missions, such as MMS, may be much larger than 10 meters to a side, even approaching 10's of kilometers. The 10% cutoff ensures that error boxes of up to half the baseline are acceptable. In an actual mission, it is unlikely that error boxes would be large enough to impact the linearization validity, because it would allow the regularity of the tetrahedron geometry (*i.e.,* the science data quality) to be significantly diminished.

IV. Model Predictive Control Using GVEs

Reference 5 showed that given a valid set of linearized dynamics and a desired trajectory, a model predictive controller for a spacecraft formation can be designed that allows for arbitrarily many convex terminal and intermediate state conditions, as well as sensor noise robustness requirements. This controller is implemented on each spacecraft in the formation and it is using a linear programming formulation. The general form of the optimization performed by the controller is

$$\min \|\mathbf{u}\|_1 \quad \text{subject to} \quad \mathbf{A}\mathbf{u} \leq \mathbf{b} \tag{19}$$

where $\mathbf{u}$ is a vector of potential control inputs and the matrix $\mathbf{A}$ and the vector $\mathbf{b}$ are formed based on the input dynamics and problem constraints.

In order to use the linearized GVE-based dynamics developed in Eq. 13 in the MPC formulation, the dynamics are discretized using a zero order hold assumption according to the procedure described in Ref. 4 yielding the discrete form

$$\zeta_i(k+1) = A_d^*(\mathbf{e}_{di})\zeta_i(k) + B_d(\mathbf{e}_{di})\mathbf{u}_i(k) \tag{20}$$

where k is the current time step, $A_d^*(\mathbf{e}_{di})$ is the system's parameter-varying state transition matrix, and $B_d(\mathbf{e}_{di})$ is the discretized form of the linearized GVE control input matrix $B(\mathbf{e}_{di})$.

V. Comparison to Another GVE-based Impulsive Control Scheme

Section II describes a number of GVE-based control schemes. The controllers based on impulsive approaches are those presented in Ref. 8 and Ref. 14. The single-thrust controller in Ref. 8 is restricted to use in LEO and can only control semimajor axis, eccentricity, and inclination. Ref. 14 describes a controller which uses four impulses over the course of an orbit to correct arbitrary orbital element perturbations. Because of its more general applicability, this section will compare the 4-impulse approach to the MPC-based approach presented in Section IV. Both schemes are designed to drive the elements of a state error ζ_i to zero over a fixed time interval. The four-impulse approach has not been presented in the context of performance criteria (*e.g.,* trajectory or terminal error boxes, robustness to disturbances) or constraints (*e.g.,* maximum thrust level), so the comparisons in this section will use an MPC controller formulation that minimizes fuel use while driving the error state to zero in a fixed time and has no other constraints.

The 4-impulse approach developed in Ref. 14 can be summarized in four steps to be taken over the course of an orbit. When the angle of latitude, θ, is 0 or π radians, implement a velocity change (impulsive thrust), Δv_{h_i} in the cross-track direction of an LVLH frame centered on the spacecraft to cancel the inclination error component of ζ_i

$$\Delta v_{h_i} = \frac{h}{r\cos\theta}\Delta i$$

When the angle of latitude, θ, is $\pi/2$ radians, implement a velocity change, Δv_{h_Ω} in the cross-track direction to cancel the ascending node error

$$\Delta v_{h_\Omega} = \frac{h\sin i}{r\sin\theta}\Delta\Omega$$

At perigee and apogee, implement Δv_{r_p} and Δv_{r_a}, respectively, in the radial direction to cancel the argument of perigee and mean anomaly errors

$$\Delta v_{r_p} = -\frac{na}{4}\left(\frac{(1+e)^2}{\eta}(\Delta\omega + \Delta\Omega\cos i) + \Delta M\right) \qquad \Delta v_{r_a} = \frac{na}{4}\left(\frac{(1-e)^2}{\eta}(\Delta\omega + \Delta\Omega\cos i) + \Delta M\right)$$

Also at perigee implement Δv_{θ_p} and at apogee implement Δv_{θ_a} in the in-track direction, to cancel the semimajor axis and eccentricity errors

$$\Delta v_{\theta_p} = \frac{na\eta}{4}\left(\frac{\Delta a}{a} + \frac{\Delta e}{1+e}\right) \qquad \Delta v_{\theta_a} = \frac{na\eta}{4}\left(\frac{\Delta a}{a} - \frac{\Delta e}{1-e}\right)$$

Using the notation and the HEO reference orbit from Section III, the following example compares the MPC method with the control approach reviewed in this section. For the state error

$$\zeta_1 = \begin{pmatrix} 10^{-9} & 10^{-7} & 10^{-7} & 10^{-7} & 10^{-7} & 10^{-7} \end{pmatrix}^T \tag{21}$$

the 4-impulse method requires 1.42 mm/s of fuel to correct the state error over the course of an orbit and the MPC method requires 0.549 mm/s of fuel. For this example, the model predictive controller was given a full orbit time horizon. However, the same control objective could have been achieved in less time, but using more fuel.

A series of 1000 orbital element state error vectors, ζ_i, were generated in which each perturbed element was a random number between $\pm 10^{-6}$. For each of the error vectors, both control methods were used to generate plans for eliminating the error. On average, the MPC maneuvers only required 51% of the fuel required by the 4-impulse maneuver.

VI. General Drift-free Tetrahedron Initial Conditions

The MMS mission will require spacecraft to form very large tetrahedron shapes, while simultaneously not drifting with respect to one another. Drift-free designs based on Hill's and Lawden's equations are valid only for formations with short baselines, because of the linearization assumptions inherent in the specification of the frames in the derivation of the dynamics. For any group of spacecraft, a no-drift requirement is equivalent to requiring that all spacecraft have the same orbital energy, which is also equivalent to stating that all spacecraft have the same semimajor axis. For a formation specified in differential orbital elements, this is the same as requiring that the desired differential semimajor axes for all spacecraft in the formation be

zero. Thus, in differential orbital elements it is trivial to design a drift-free formation, however, the curvilinear nature of the elements makes describing and manipulating general tetrahedron shapes complicated.

One approach is to begin with tetrahedron coordinates in a rectilinear frame (such as LVLH or ECEF) and then convert those coordinates into orbital element perturbations. However, producing the desired orbital element differences for a tetrahedron requires knowledge of the full relative state in a rectilinear frame, including both position and velocity. If the only constraint on the formation geometry is that the satellite positions form a tetrahedron shape, then the velocity must be selected based on additional criteria.

A regular tetrahedron with sides of length s can be described in a rectilinear frame using the coordinates (given in x, y, z triples)

$$\text{Sat}_1 = (0, 0, \frac{\sqrt{3}}{3}s) \qquad \text{Sat}_2 = (0, \frac{1}{2}s, -\frac{\sqrt{3}}{6}s) \qquad \text{Sat}_3 = (0, -\frac{1}{2}s, -\frac{\sqrt{3}}{6}s) \qquad \text{Sat}_4 = (\frac{\sqrt{6}}{3}s, 0, 0)$$

If the rectilinear frame is LVLH, the coordinates can be transformed into differential orbital elements using the first order approximation

$$\delta\mathbf{e}_{di} = M(\mathbf{e}_1)\mathbf{x}_{di} \tag{22}$$

where $\mathbf{e}_1$ is the reference orbit that the differential elements of the vector $\delta\mathbf{e}_{di}$ are described with respect to, and $\mathbf{x}_{di}$ is a relative state vector in the LVLH frame centered on the absolute orbit $\mathbf{e}_1$. The elements of the 6×6 rotation matrix $M(\mathbf{e}_1)$ are known analytically and can be found in Appendix G of Ref. 13. It should be noted that these projections from LVLH coordinates to differential orbital elements can be used to establish three and six dimensional "box" constraints on spacecraft position and velocity of the type discussed in Refs. 5 and 24.

The desired LVLH state of satellite i can be expressed as the concatenation of a position vector $\mathbf{p}_i$ and a velocity vector $\mathbf{v}_i$, each with states in the x, y, and z directions.

$$\mathbf{x}_i = \begin{pmatrix} \mathbf{p}_i^T & \mathbf{v}_i^T \end{pmatrix}^T = \begin{pmatrix} x_i & y_i & z_i & v_{x_i} & v_{y_i} & v_{z_i} \end{pmatrix}^T \tag{23}$$

To find velocity vectors that satisfy the no-drift requirement, the system

$$\delta\mathbf{e}_{di} = M(\mathbf{e}_1)\begin{pmatrix} \mathbf{p}_{di} \\ \mathbf{v}_{di} \end{pmatrix} \quad \forall \;\; i = 1\ldots n \tag{24}$$

must be solved with the additional constraint that the semimajor axis element of $\delta\mathbf{e}_{di}$ be equal to zero for all spacecraft in the formation ($n = 4$ for a tetrahedron formation). In this system, the elements of $\delta\mathbf{e}_{di}$ and $\mathbf{v}_i$ are allowed to vary, while the matrix M and the vectors $\mathbf{x}_i$ are determined by the reference orbit and the tetrahedron geometry, respectively. The system has $9n$ variables and $7n$ constraints and will, therefore, have many possible solutions. In Ref. 18, the velocity magnitude is chosen to achieve the no-drift condition and the ECI velocity direction of each spacecraft in the formation is chosen to match the direction of reference orbit's velocity vector. This method will succeed in creating a drift-free formation, however it does not take into account the states of the spacecraft in the formation immediately prior to initialization.

The approach presented here minimizes the size of the maneuvers that would be required to create the desired formation. The approach selects initial conditions, $\delta\mathbf{e}_{di}$, that are closest to the current differential states, $\delta\mathbf{e}_i$, of the spacecraft in the formation and that will minimize the state error, ζ_i, across the formation at the start of the initialization. For the entire formation, this criterion becomes

$$\min_{\delta\mathbf{e}_{di},\mathbf{v}_{di} \;\forall i=1\ldots n} \sum_{i=1}^{n} \|W_i(\delta\mathbf{e}_{di} - \delta\mathbf{e}_i)\|_1 \tag{25}$$

where W_i are weighting matrices that represent the expected fuel-cost of changing orbital elements (obtainable from the GVEs). Allowing different W_i for each spacecraft enables the formation design to take into account factors such as fuel-weighting to extend overall mission duration, similar to the approach used in choosing the *virtual center* in Section VII. The use of a 1-norm is appropriate in this case, because the distance that a given element must be changed is the absolute value of the difference between that element's current and desired state. This approach is similar to the optimization used in Ref. 3, in which drift-free, minimum maneuver constants of integration were found for Lawden's Equations. Next, the optimization is expanded by exploiting specific aspects of the MMS mission science goals.

The *quality* of the shape of the regular tetrahedron[a] largely determines the value of the science data recovered by a mission such as MMS.[19] In choosing the initial conditions for a regular tetrahedron-shaped

[a]Tetrahedron quality is discussed in Ref. 24

formation, certain quantities that do not affect shape quality such as the scale, position, and orientation of the tetrahedron can be considered degrees of freedom in the optimization described by Eqs. 24 and 25. By optimizing the additional degrees of freedom, tetrahedron-shaped initial conditions can be found that require smaller maneuvers to achieve from the current formation state. Scaling the tetrahedron shape equally in three dimensions introduces a single scalar variable s and allowing translation in each orthogonal direction of the LVLH frame introduces the variables t_x, t_y, and t_z. The new constraint set is

$$\delta\mathbf{e}_{di} = M(\mathbf{e}_1)\left[\begin{pmatrix} s\mathbf{p}_{di} \\ \mathbf{v}_{di} \end{pmatrix} + \mathbf{t}\right] \quad , \quad \begin{pmatrix} 1 & 0 & 0 & 0 & 0 & 0 \end{pmatrix}\delta\mathbf{e}_{di} = 0 \qquad \forall \;\; i = 1\ldots n \tag{26}$$

where $\mathbf{t} = \begin{pmatrix} t_x & t_y & t_z & 0 & 0 & 0 \end{pmatrix}^T$ and the second constraint forces a no-drift condition by ensuring that the relative semimajor axes, the first element of each $\delta\mathbf{e}_{di}$ vector, are zero. These constraints can be combined with the objective in Eq. 25 and formulated as a linear program. In addition to the geometric and no-drift constraints, limits on the desired differential angle state variables are required to ensure that they remain within $\pm\pi$ and on eccentricity and semimajor axis to ensure that the spacecraft remain in Earth orbit.

For elliptical orbits, it is not possible to maintain constant relative geometry between satellites for all points in the orbit. Instead, a single position in the orbit must be chosen for the satellites to form a tetrahedron. The mean anomaly at the time of the tetrahedron geometry will be M_t. When formulating the optimization in Eqs. 25 and 26, the current differential element vectors ζ_i must be propagated forward using the A^* matrix in Eq. 9 to the mean anomaly M_t. In addition, the reference orbit used to compute the matrix $M(\mathbf{e}_1)$ should have a mean anomaly set to M_t.

There are several limitations to this optimization approach. First, it does not optimally assign spacecraft to positions in the tetrahedron (a formulation that does this is possible using mixed integer linear programming or network LP[5, 21]). Second, the optimization posed here does not optimally orient the tetrahedron in three space. Introducing a rotation matrix dependent on three Euler parameters would create a nonlinear optimization. This limitation could be bypassed by creating a spherical lattice about the orbit and optimizing the formation rotated once for each point on the lattice. After performing all the optimizations, the desired state corresponding to the rotation with the lowest cost would be chosen. Although this approach requires a preset number of optimizations (possibly many depending upon the degree of rotation resolution desired), the optimizations are small linear programs, which complete in a fraction of a second.

An alternative form of Eq. 26 can be written to allow for small rotations using the linearized form of a three-dimensional rotation matrix[17]

$$\mathbf{x}' = \begin{pmatrix} 1 & \theta_z & -\theta_y \\ -\theta_z & 1 & \theta_x \\ \theta_y & -\theta_x & 1 \end{pmatrix}\mathbf{x} \equiv \mathbf{R}\mathbf{x} \tag{27}$$

where θ_x is the rotation about the x axis, θ_y is the rotation about the y axis, θ_z is the rotation about the z axis, $\mathbf{x}$ is an arbitrary LVLH position vector, and $\mathbf{x}'$ is the vector $\mathbf{x}$ after having been rotated. Using Eq. 27 in Eq. 26 yields

$$\delta\mathbf{e}_{di} = M(\mathbf{e}_1)\left[\begin{pmatrix} \mathbf{R} & \mathbf{0}_3 \\ \mathbf{0}_3 & \mathbf{I}_3 \end{pmatrix}\begin{pmatrix} \mathbf{p}_{di} \\ \mathbf{v}_{di} \end{pmatrix} + \mathbf{t}\right] \quad , \quad \begin{pmatrix} 1 & 0 & 0 & 0 & 0 & 0 \end{pmatrix}\delta\mathbf{e}_{di} = 0 \qquad \forall \;\; i = 1\ldots n \tag{28}$$

where $\mathbf{R}$ is the rotation matrix defined in Eq. 27, $\mathbf{0}_3$ is a 3×3 matrix of zeros, and $\mathbf{I}_3$ is a 3×3 identity matrix. The variables being chosen in the new optimization are the vectors $\delta\mathbf{e}_{di}$, the rotations θ_x, θ_y, and θ_z (contained in $\mathbf{R}$), the velocities $\mathbf{v}_{di}$, and the translations $\mathbf{t}$. The optimization can perform small rotations (θ_x, θ_y, and θ_z are constrained), but can no longer optimize the tetrahedron scale and still retain linearity.

Example: Fuel Expenditure for Rotation Approach – Using the highly elliptical orbit from the example in Section III, the initial conditions for a tetrahedron with 1000 kilometer sides were found using the optimization criterion in Eq. 25 and the constraints in Eq. 28 and Eq. 26. It was assumed that the four satellites began from the near-tetrahedron configuration

$$\begin{pmatrix} \delta\mathbf{e}_1^T \\ \delta\mathbf{e}_2^T \\ \delta\mathbf{e}_3^T \\ \delta\mathbf{e}_4^T \end{pmatrix}^T = \begin{pmatrix} 0.00000051246464 & 0.000000037450312 & 0.00000055474668 & 0.00000071331420 \\ 0.000013574046 & -0.000014775678 & 0.0000023691051 & 0.019396998 \\ 0.00000069359286 & 0.00000096599445 & 0.00000031827579 & 0.00000025502725 \\ 0.043440693 & -0.021683522 & -0.021758507 & -0.000062072563 \\ 0.00000046215002 & 0.00000015393732 & 0.00000045211263 & 0.00000013838810 \\ -0.24535033 & -6.1230191 & -6.1975472 & -6.2827584 \end{pmatrix} \tag{29}$$

Table 1: Maneuver Cost: Tetrahedron Initial Condition Optimization

DOF	SC 1	SC 2	SC 3	SC 4	Initialization Total
No Rotation No Translation	51.3[b]	193	213	6.487×10^6	6.487×10^6
No Rotation Translation: ±1 km	127	246	161	299	833
No Rotation Scaling: ±5%, Translation: ±1 km	101	423	0.430	202	726
Rotation: ±0.1 radians No Translation	8.316	7.696	5.846	1.484	23.342
Rotation: ±0.1 radians Translation: ±1 km	2.422	0.669	1.080	1.199	5.370

When computing the objective function for this example, the spacecraft state errors and individual elements were weighted equally. Table 1 shows the results of several optimizations, each with different degrees of freedom enabled. The table shows that the most significant fuel advantage is achieved through the combination of rotation and translation. In the rotation/translation combination, the optimization created the desired differential elements

$$\begin{pmatrix} \delta\mathbf{e}_{d1}^T \\ \delta\mathbf{e}_{d2}^T \\ \delta\mathbf{e}_{d3}^T \\ \delta\mathbf{e}_{d4}^T \end{pmatrix}^T = \begin{pmatrix} 0.0 & 0.0 & 0.0 & 0.0 \\ 0.00001431718302 & -0.00001477567840 & 0.000002369105057 & 0.01939715857 \\ 0.0000006935928587 & 0.0000009659944468 & 0.0000003182757864 & 0.0000002550272544 \\ 0.04344069265 & -0.02168323583 & -0.02175888889 & -0.00006175523238 \\ 0.0000004621762758 & 0.0000001534168443 & 0.0000004519745972 & 0.0000001381876841 \\ -0.2453529547 & -6.123019124 & -6.197547224 & -6.282758434 \end{pmatrix} \tag{30}$$

where the limits of the translation variables are ± 1 km and the limits of the three rotation variables were each ±0.1 radians. Within those limits, the optimal translation and rotation vectors were found to be

$$\mathbf{t} = \begin{pmatrix} 26.809 & 52.500 & -6.344 \end{pmatrix}^T \tag{31}$$

$$\begin{pmatrix} \theta_x & \theta_y & \theta_z \end{pmatrix}^T = \begin{pmatrix} -0.001005 & -0.000997 & -0.0007217 \end{pmatrix}^T \tag{32}$$

in meters and radians. The planner described in Section IV was used to create the formation geometries specified in Eq. 30 from the initial conditions specified in Eq. 29. The total maneuver fuel cost to create the formation (*i.e.,* the sum of the costs for each spacecraft) was 6.33 mm/s.

VII. Formation Flying: Coordination Using GVEs

The model predictive controller described in Section IV is designed to be decentralized, with a fully independent controller being run on each spacecraft. The controller designs trajectories that will keep a spacecraft i inside an error box centered about the spacecraft's desired orbit, $\mathbf{e}_{di}$. In Section III, the desired orbits are defined with respect to the actual orbit of an arbitrary satellite in the formation, $\mathbf{e}_1$, using differential orbital element vectors, $\delta\mathbf{e}_{di}$, in the same manner used in Ref. 13. Section VI presented an approach for choosing initial conditions that minimized the weighted state error across the formation. In a system where initial conditions are chosen infrequently, it may be desirable to introduce additional coordination into the formation. When spacecraft each track desired states with no coordination, the control task is referred to as *formation-keeping*.[5] Alternately, *formation flying* occurs when the spacecraft controllers collaborate to achieve formation-wide fuel minimization. This coordination can be achieved by calculating a central point that minimizes the overall weighted state error of each spacecraft in the formation. Approaches to implementing closed-loop coordination of this type are presented in Refs. 11 and 22. The *virtual center* approach in Ref. 11 is a centralized calculation of the error-minimizing center based on fuel-weighting and derived from measurements available through carrier-phase differential GPS (CDGPS) relative navigation

[b]Fuel use indicated in mm/s

of the type described in Ref. 23. An equivalent approach can be used to find an error-minimizing reference orbit for a formation described in differential orbital elements.

Measurements from a CDGPS relative navigation system are assumed to be in the form of relative LVLH states 23, $\mathbf{x}_i$, for each satellite in the formation. The measurements will be relative to an arbitrary absolute satellite state, $\mathbf{e}_1$, in the formation, which is assumed to be at the origin of the LVLH frame. In addition to relative states, the GPS sensors on each satellite can be expected to compute a less accurate estimate of the spacecraft's absolute state. Given an estimate of the absolute state in Earth Centered Inertial (ECI) coordinates, $\mathbf{X}_{\mathrm{ECI}_1}$ and the relative states $\mathbf{x}_i$, the differential states $\delta\mathbf{e}_i$ in Eq. 4 can be computed in several ways. The matrix $M(\mathbf{e}_1)$ from Eq. 22 could be computed and used to create a first order approximation of the relative differential element states. However, an exact conversion can be calculated by forming estimates of the absolute states of each of the satellites based on their relative measurements

$$\mathbf{X}_{\mathrm{ECI}_i} = \mathbf{X}_{\mathrm{ECI}_1} + \mathbf{x}_i \tag{33}$$

The absolute states $\mathbf{X}_{\mathrm{ECI}_i}$ can be converted to Keplerian orbital elements, $\mathbf{e}_i$, of each satellite using a well-known procedure described in Ref. 1. The relative measurements are then recovered in terms of differential orbital elements, $\delta\mathbf{e}_i$, using Eq. 4. Desired differential elements, $\delta\mathbf{e}_{dci}$, are then specified with respect to an unknown virtual center state, $\delta\mathbf{e}_c$, which is specified with respect to the absolute state $\mathbf{e}_1$. Using the procedure described in Ref. 11, the error of a spacecraft with respect to the virtual center, ζ_{ci} is given by

$$\mathbf{e}_i - \delta\mathbf{e}_{dci} - \delta\mathbf{e}_c = \zeta_{ci} \tag{34}$$

which can be placed in the standard least squares form $b_i - A_i\delta\mathbf{e}_c = \zeta_{ci}$, where $b_i = \mathbf{e}_i - \delta\mathbf{e}_{dci}$, A_i is a 6×6 identity matrix, and $\delta\mathbf{e}_c$ denotes the location of the virtual center with respect to $\mathbf{e}_1$ in differential orbital elements. By concatenating the b_i, A_i, and ζ_{ci} vectors for each spacecraft, the statement of error for the entire formation is written $b - A\delta\mathbf{e}_c = \zeta$, where $b = (\ b_1 \quad \dots \quad b_n\ )^T$, $A = (\ A_1 \quad \dots \quad A_n\ )^T$, and $\zeta = (\zeta_{c1} \ \dots \ \zeta_{cn})^T$. The solution that minimizes the error vectors globally in a weighted least squares sense is

$$\delta\mathbf{e}_c = (A^T W A)^{-1} A^T W b \tag{35}$$

where W is a weighting matrix that can be used to bias the center location according to the fuel-use rates of different satellites in the formation, as well as to weight orbital elements individually based upon the amount of control required to alter them (obtainable from the GVEs for $\mathbf{e}_1$).

VIII. Decentralization of Virtual Center Scheme

The virtual center calculation in Eq. 35 is the well-known closed-form solution to a least squares problem. The solution to the decentralized least-squares problem is also readily available in the literature and is given for spacecraft i as

$$\delta\mathbf{e}_{c_i} = \delta\mathbf{e}_{c_{i-1}} + (A^T\bar{W}_i A)^{-1} A_i^T W_i (b_i - A_i\delta\mathbf{e}_{c_{i-1}}) \quad \forall \quad i = 1 \dots n \tag{36}$$

where $A = (\ A_1 \quad \dots \quad A_i\ )^T$ and $\bar{W}_i = \mathrm{diag}\ (W_1, \dots, W_i)$. This decentralized procedure would begin with an initial estimate $\delta\mathbf{e}_{c_1} = b_1$ and spacecraft i would pass both $\bar{W}_i$ and $\delta\mathbf{e}_{c_i}$ on to the next spacecraft $(i+1)$ in the formation. The estimate of the virtual center, $\delta\mathbf{e}_n$ will then be equal to the fully centralized solution, which could be broadcast back to the entire formation.

The decentralized calculation can be simplified using several reasonable assumptions. First, assume that the relative weighting between differential orbital elements is the same for all spacecraft and is calculated to be W_e based on the absolute orbit $\mathbf{e}_1$, which is known by all spacecraft in the formation. Next, let the fuel-based weighting for each spacecraft be represented by a scalar, w_i. Now, the total weighting matrix, W_i, for each spacecraft is given by

$$W_i = w_i W_\mathrm{e} \quad \forall \quad i = 1 \dots n \tag{37}$$

Also assume that the variable being solved for is always the exact virtual center, $\delta\mathbf{e}_c$, making the A_i matrix for each satellite a 6×6 identity matrix. Now, for the ith satellite $W = \mathrm{diag}\ (w_1 W_\mathrm{e}, \dots, w_i W_\mathrm{e})$, and A is a column of i concatenated 6×6 identity matrices. The decentralized solution for the ith satellite

becomes

$$\begin{aligned}\delta\mathbf{e}_{c_i} &= \delta\mathbf{e}_{c_{i-1}} + (A^T W A)^{-1} A_i^T W_i (b_i - A_i \delta\mathbf{e}_{c_{i-1}}) \\ &= \delta\mathbf{e}_{c_{i-1}} + w_i \left(\begin{bmatrix} I & \dots & I \end{bmatrix} \begin{bmatrix} w_1 W_\mathrm{e} & 0 & \dots & 0 \\ 0 & w_2 W_\mathrm{e} & \dots & 0 \\ \vdots & 0 & \ddots & 0 \\ 0 & 0 & \dots & w_i W_\mathrm{e} \end{bmatrix} \begin{bmatrix} I \\ I \\ \vdots \\ I \end{bmatrix} \right)^{-1} W_\mathrm{e}(b_i - \delta\mathbf{e}_{c_{i-1}})\end{aligned} \tag{38}$$

which can be further simplified to

$$\delta\mathbf{e}_{c_i} = \delta\mathbf{e}_{c_{i-1}} + w_i[(w_1 + \ldots + w_i)W_\mathrm{e}]^{-1} W_\mathrm{e}(b_i - \delta\mathbf{e}_{c_{i-1}}) = \delta\mathbf{e}_{c_{i-1}} + \frac{w_i}{w_1 + \ldots + w_i}(b_i - \delta\mathbf{e}_{c_{i-1}}) \tag{39}$$

Introducing $\bar{w}_i$, the sum of all previous scalar weights $\bar{w}_i = \sum_{k=1}^{i} w_k$, the new recursion becomes

$$\delta\mathbf{e}_{c_i} = \delta\mathbf{e}_{c_{i-1}} + \frac{w_i}{\bar{w}_{i-1} + w_i}(b_i - \delta\mathbf{e}_{c_{i-1}}) \tag{40}$$

and the only information that needs to be passed to the next spacecraft to form $\delta\mathbf{e}_{c_{i+1}}$ is the current virtual center estimate, $\delta\mathbf{e}_{c_i}$, and the scalar $\bar{w}_i$.

IX. Formation Maintenance on MMS-like Mission

The control system described in Section IV was demonstrated on a segment of the MMS mission. The MMS mission is comprised of four spacecraft that create regular tetrahedron geometries once per orbit. The orbits of the four spacecraft are widely separated and highly elliptical, presenting a challenge for many optimal formation specification and control approaches in the literature.[2,3] Using the tetrahedron initial-condition optimization approach in Section VI and the model predictive approach in Section IV, the four spacecraft were controlled in a fully nonlinear simulation with atmospheric drag effects (unmodeled oblateness disturbances were not used) using a commercial orbit propagator. Figure 3 shows the rate at which fuel was used over the course of two weeks of formation flying. After an initial transient period, the formation fuel use rate converges to approximately 5.95 mm/s per day (≈ 1 orbit) for each satellite.

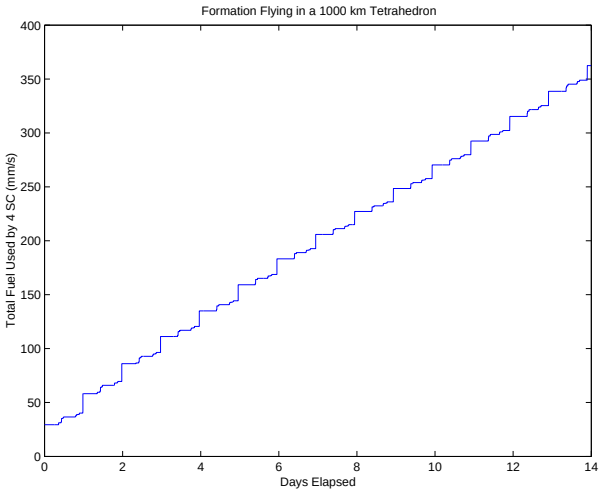

Fig. 3: Fuel cost for maintaining a 1000 km tetrahedron formation in a highly eccentric orbit

X. Conclusion

Gauss' Variational Equations have been used to derive a set of linearized relative dynamics of orbital motion. Using a linear parameter varying dynamics model, such as GVEs, for control allows a compromise between simple but inaccurate linear models (e.g., Hill's equations) and high fidelity but difficult to control nonlinear models. The linearization assumptions for the new set of dynamics were shown to be valid for typical spacecraft error box sizes. The linearized GVE-based dynamics were used in a model predictive controller of the form described in Ref. 5 and the combination is shown to be more fuel-efficient than an impulsive based (non-optimized) GVE technique. By combining differential element orbit specifications and dynamics linearized about the spacecraft in the formation, the problems of long-baseline initialization and control discussed in Ref. 24 are eliminated.

A method of specifying differential orbital elements for a desired formation geometry was introduced which optimizes the parameters in the initialization problem to minimize the fuel required to maneuver into the new formation. This method was applied to a regular tetrahedron-shaped orbit of the type planned for the MMS mission. A method of applying rectilinear error box constraints to a formation specified in differential orbital

elements was also presented. Finally, the virtual center approach for coordinating spacecraft formations[11] was formulated in terms of the differential orbital elements, and a means of decentralizing the algorithm was shown. The GVE-based dynamics/MPC controller was used to specify and control a tetrahedron-shaped formation in an MMS-like orbit for a period of two weeks.

Acknowledgments

This work was funded under NASA Grant NAG5-10440 and Cooperative Agreement NCC5-729 through the NASA GSFC Formation Flying NASA Research Announcement. Any opinions, findings, and conclusions or recommendations expressed in this material are those of the author(s) and do not necessarily reflect the views of the National Aeronautics and Space Administration.

References

[1]M. Kaplan. *Modern Spacecraft Dynamics and Control*. Wiley, 1976.

[2]M. Tillerson and J. How, "Formation Flying Control in Eccentric Orbits," *Proceedings of the AIAA Guidance, Navigation, and Control Conference*, Montreal, Canada, Aug. 6-9, 2001, Collection of Technical Papers, Reston, VA, American Institute of Aeronautics and Astronautics, 2001.

[3]G. Inalhan, M. Tillerson, and J. How, "Relative Dynamics & Control of Spacecraft Formations in Eccentric Orbits," AIAA Journal of Guidance, Control, and Dynamics (0731-5090), vol. 25, no. 1, Jan.-Feb. 2002, p. 48-59.

[4]G. Franklin, J. Powell, and M. Workman, "Digital Control of Dynamic Systems," Third Edition,Addison-Wesley, 1998.

[5]M. Tillerson, G. Inalhan, and J. How, "Coordination and Control of Distributed Spacecraft Systems Using Convex Optimization Techniques," Int. Journal of Robust and Nonlinear Control, vol 12, Issue 2-3, Feb.-Mar. 2002, p.207-242.

[6]Ilgen, M.R., "Low Thrust OTV Guidance using Lyapunov Optimal Feedback Control Techniques," AAS/AIAA *Astrodynamics Specialist Conference*, Victoria, B.C., Canada, Aug. 16–19 1993, Paper No. AAS 93-680.

[7]B. Naasz, *Classical Element Feedback Control for Spacecraft Orbital Maneuvers,* S.M. Thesis, Dept. of Aerospace Engineering, Virginia Polytechnic Institute and State University, May 2002.

[8]Mishne, D. "Formation Control of LEO Satellites Subject ot Drag Variations and J_2 Perturbations," AAS/AIAA Astrodynamics Specialist Conference, Monterey, California, August 2002.

[9]P. Gurfil, "Control-Theoretic Analysis of Low-Thrust Orbital Transfer Using Orbital Elements," *AIAA Journal of Guidance, Control, and Dynamics*, vol. 26, no. 6, November-December 2003, p. 979-983.

[10]T.E. Carter and S.A. Alvarez, "Quadratic-Based Computation of Four-Impulse Optimal Rendezvous near Circular Orbit," *AIAA Journal of Guidance, Control, and Dynamics*, vol. 23, no. 1, January-February 2000, p. 109-117.

[11]M. Tillerson, L. Breger, and J. How, "Distributed Coordination and Control of Formation Flying Spacecraft," Proceedings of *American Control Conference*, June 2003.

[12]K. T. Alfriend, H. Schaub, and D.-W. Gim, "Formation Flying: Accomodating Non-linearity and Eccentricity Perturbations," presented at the 12th *AAS/AIAA Space Flight Mechanics Meeting,* January 27-30, 2002.

[13]H. Schaub and J.L. Junkins, *Analytical Mechanics of Space Systems,* AIAA Education Series, Reston, VA, 2003.

[14]H. Schaub and K. Alfriend, "Impulsive Feedback Control to Establish Specific Mean Orbit Elements of Spacecraft Formations," *AIAA Journal of Guidance, Control, and Dynamics*, vol. 24, no. 4, July-Aug. 2001, p. 739-745.

[15]L. Mailhe, C. Schiff, and S. Hughes, "Formation Flying in Highly Elliptical Orbits: Initializing the Formation," *Proceedings of the International Symposium on Space Dynamics,* Biarritz, France, CNES, June 26-30, 2000. Paper MS00/21.

[16]Battin, Richard H., *An Introduction to the Mathematics and Methods of Astrodynamics,* AIAA Education Series, New York, 1987.

[17]Greenwood, D.T., *Advanced Dynamics,* Cambridge University Press, Cambridge, 2003.

[18]J. Guzman and C. Schiff, "A Preliminary Study for a Tetrahedron Formation (Spacecraft Formation Flying)," *AIAA/AAS Astro. Specialists Conf.*, Aug 2002.

[19]P. Robert, A. Roux, C. Harvey, M. Dunlop, P. Daly, and K. Glassmeier, "Tetrahedron Geometric Factors," Analysis Methods for Multi-Spacecraft Data, pp. 323348, Noordwijk, The Netherlands: ISSI Report SR-001, ESA Pub. Div., 1998.

[20]S. Curtis, "The Magnetospheric Multiscale Mission Resolving Fundamental Processes in Space Plasmas," NASA GSFC, Greenbelt, MD, Dec. 1999. NASA/TM2000-209883.

[21]D. Bertsimas and J.N. Tsitsiklas, *Introduction to Linear Optimization,* Athena Scientific, Belmont, 1997.

[22]W. Ren, and R. Beard, "Virtual Structure Based Spacecraft Formation Control with Formation Feedback," presented at the *AIAA GN&C Conference,* Aug. 2002.

[23]F. Busse, J. How, J. Simpson, and J. Leitner, "PROJECT ORION-EMERALD: Carrier Differential GPS Techniques and Simulation for Low Earth Orbit Formation Flying," presented at the *IEEE Aerospace Conference*, Mar 10-17, 2001.

[24]L.S. Breger, *Model Predictive Control for Formation Flying Spacecraft*, S.M. Thesis, Massachusetts Institute of Technology, Dept. Aeronautics and Astronautics, June 2004.